Int. J. Nanosci. Nanotechnol., Vol. 11, No. 1, March 2015, pp. 1-12

Upgrading TiO_2 Photoactivity under Visible Light by Synthesis of MWCNT/TiO_2 Nanocomposite

E. Soroodan Miandoab and Sh. Fatemi*

School of Chemical Engineering, University College of Engineering, University of Tehran, Enghelab Street, P.O.Box 11365-4563, Tehran, I.R.Iran

(*) Corresponding author: shfatemi@ut.ac.ir
(Received: 31 Dec 2014 and Accepted: 17 Feb. 2015)

Abstract:

Nanocomposites of multi-walled carbon nanotubes and titanium dioxide (MWCNT/TiO_2) were synthesized by the sol-gel method. Regarding hydrophobicity of carbon nanotubes (CNTs), benzyl alcohol was used as the linking agent between CNT powder and TiO_2 gel which was prepared from the precursor of titanium tetraisopropoxide. The prepared samples were treated under thermal treatments. A part of the samples was heated to prepare MWCNT/TiO_2 nanocomposite with anatase TiO_2 and the other parts were heated until burning CNTs and prepare pseudo-tube TiO_2 (PT-TiO_2). The materials were characterized by field emission scanning electron microscopy (FESEM), X-ray diffraction (XRD), thermo gravimetric analysis (TGA), Brunauer-Emmet-Teller (BET) measurement and UV-vis diffuse reflectance spectra (DRS). The photocatalytic activity of MWCNT/TiO_2 and PT-TiO_2 was studied for degradation of acetaldehyde under UV-visible and visible light irradiation. The Photocatalytic reaction was examined in a gaseous stirred flow reactor equipped with 80W Hg lamp and the concentration–time results were compared with commercial TiO_2 (P25-TiO_2). Considerable reduction of acetaldehyde concentration was achieved under visible irradiation by the MWCNT/TiO_2 nanocomposite, whereas none of the PT-TiO_2 and typical P25-TiO_2 showed activity under visible light. An optimal fraction of 30 wt% MWCNT in anatase TiO_2 was found to have the highest activity under visible light irradiation.

Keywords*: MWCNT/TiO_2 Nanocomposite, Photocatalytic activity, Pseudo-tube TiO_2, Visible light*

1. INRODUCTION

Decomposition of pollutants by photoactive catalysts under normal temperatures and pressures is a promising process to tackle some of environmental issues and to get toward clean energy technologies. TiO_2 is the most investigated photocatalysts due to its chemical stability, long durability, nontoxicity, low cost and sensitivity toward irradiation [1]. However, wide band gap of anatase (3.2 eV) requires UV light radiation for activation. In addition, high recombination rate of electron-hole pairs is another disadvantage of the photocatalytic activity [2]. Many admirable efforts have been fulfilled to create visible light active TiO_2 photocatalysts and they have already been well reviewed by Pelaez *et al*. [3].

Mixed-phase TiO_2 composites tend to show higher photoactivity than pure-phase materials, due to the formation of solid–solid interfaces that facilitates charge transfer and separation, reduce electron–hole recombination and interfacial

defect sites that can act as catalytic hot spots. Since mid-1990s, attention to the carbonaceous materials has been grown because of their unique structural and compositional properties [4]. Among carbonaceous materials, CNT has found considerable attractions that can act as a support or hard template to extend electron-hole recombination time as electron scavengers [5]. Several advantages of CNTs in hybrid materials include their high aspect ratio (>1000) and tubular geometry provide ready gas access to a large specific surface area and percolation at very low volume fractions. Their excellent mechanical, electrical and optical properties support CNTs as an ideal building block in hybrid materials. The high thermal conductivity of CNTs enables them to behave as a heat sink during calcinations and activation treatments, thereby stabilizing small inorganic moieties that can decorate the sidewalls of the CNTs. [6].

Several procedures have been adopted in literatures for fabrication of CNT/TiO_2 hybrid materials and evaluation of their performance in photocatalytic decomposition of organic compounds, including simple mixing [7], sol-gel method [8], hydration-dehydration technique [9], micro-emulsion [10], solvothermal [11], etc. Coupling of hydrophilic TiO_2 particles to hydrophobic surface of CNT has been the focus of considerable attention in all related investigations. To render hydrophilic nature to the surface of CNT, some modifications should be performed through organic functional groups. In general, CNTs can be functionalized by a) covalent bonding and b) non-covalent adsorption or wrapping of various functional molecules which utilizes Van der Waals or hydrogen bonding [6]. The most conventional route for covalent bonding involves acid treatment of CNTs through a mixture of H_2SO_4 and HNO_3 in which carbonyl and carboxyl groups are attached on CNTs surfaces [12]. Other covalent functionalization approaches include sidewall halogenations, hydrogenation, cycloadditions, radical addition, electrophilic additions, ozonolysis and plasma activation [13]. To distinguish the dependence of photocatalytic activity of CNT/TiO_2 nanocomposites on the modification of CNTs, Djokić *et al*. compared the photocatalytic ability of oxidized-CNT/TiO_2 with amino treated-CNT/TiO_2 under UV wavelengths and concluded better performance of oxidized CNT/TiO_2 nanocomposites [14]. Utilization of covalent bonding for CNT modification is led to random aggregation of TiO_2 on CNTs surfaces and leaves bare and uncoated CNTs [8]. This will affect the photocatalytic properties directly. Gao *et al*. comparatively studied photocatalytic efficiency of CNT/TiO_2 nanocomposites made by conventional sol-gel method via acid treated CNTs and novel "surfactant wrapping" method. The results expressed noticeable improvement in photocatalytic activity under UV irradiation for "surfactant wrapping" with respect to conventional sol-gel method [15].

Although worthwhile results have been obtained from various similar investigations, dominant researches have concentrated on photocatalytic processes under UV radiation. Also, enhancement of photocatalytic phenomenon to visible light region have not been widely studied. In addition, previous investigations have been predominantly applied for covalent bonding, i.e. traditional acid treatment of CNTs to induce hydrophilic nature to the CNTs. With these in mind, in this research, MWCNT/TiO_2 nanocomposite was prepared by a facile sol-gel method with the aiding of benzyl alcohol as a linking agent to prepare the CNTs surface for coupling with synthesized TiO_2 crystals. Functionalizing with strong oxidizing agents creates covalent bonds with the surface of CNT which is a process with little control over the nature, location, thickness and uniformity of functional groups; whereas benzyl alcohol is able to undergo π-π stacking without any covalent bond with the surface of CNT resulting homogenously coating of TiO_2 sols over the CNTs [16]. Produced MWCNT/TiO_2 nanocomposites as well as post thermal treated MWCNT/TiO_2, named PT-TiO_2, were comparatively examined for their photoactivity to VOC removal in a mixed continuous gaseous reactor under visible light irradiation. Up to now, most of prior investigations have focused on batch processes in liquid phase and under UV irradiation. Indeed, the final purpose in our research deals with upgrading electronic and optical properties of

titania to the visible light region in continuous gaseous conditions to be proposed for scaling up the photocatalytic processes.

2. MATERIAS AND METHODS

2.1. Materials

MWCNTs with 20-40 nm in diameters and one micron in length (Neutrino Co.), Ethanol (C_2H_5OH, Merck, 99% pure), Titanium tetraisopropoxide ($Ti(i\text{-}C_3H_7O_2)_4$, Panreac, 97% pure), Benzyl alcohol (C_7H_8O, Merck, 99% pure), Acetaldehyde (CH_3CHO, Merck, 99% pure) and commercial TiO_2 powder (P25 Sigma Aldrich) were used as received.

2.2. Synthesis

20, 30 or 40 wt% MWCNTs (abbreviated as NC1, NC2 and NC3) were dispersed in ethanol and vigorously stirred with the aiding of an ultrasonic bath for 30 minutes. After stirring, deionized water and benzyl alcohol (BA) were added to the suspension. Titanium tetraisopropoxide (TTIP) was dissolved in ethanol and slowly dropped into the MWCNT suspension. Added weight fractions in primary solution were selected to have a specific molar ratios of 1:30:6:3, for TTIP: ethanol: water: BA, respectively. Entire mixture was stirred for 1 hour at room temperature. Remained precipitate was filtered and dried in air at 100°C for 6 hours. The dried samples were calcined in air at 450°C for 4 hours to get desired anatase crystalline phase of TiO_2. In another part of the experiments, heat treatment of the synthesized MWCNT/TiO_2 nanocomposites was extended to the higher temperature of 550°C in an atmospheric furnace for 4 hours to remove MWCNTs that resulted in production of PT-TiO_2 structures free from MWCNTs.

2.3. Characterization techniques

Morphological characteristics of prepared materials were probed by field emission scanning electron microscopy (FESEM) using Hitachi-F4160. X-ray diffraction (XRD) patterns were collected by a Phillips diffractometer using CuKα (λ=1.54056A) radiation in angular domain of 0< 2θ< 80. To estimate CNTs content, thermogravimetric analysis was performed using NETZSCH TG 209 F1 Iris with a ramp of 20°C/min. Textural structure and specific surface areas were determined by N_2 gas adsorption-desorption isotherms and Brunauer–Emmett–Teller (BET) technique (Bellsorb mini-II). Diffuse reflectance spectra (DRS) were obtained to measure photo-absorbance data for each sample using a UV–vis spectrophotometer (model Avaspec-2048-TEC), and $BaSO_4$ was applied as a reference.

2.4. Photocatalytic experiments

The photocatalytic activity was monitored by degradation of gaseous phase acetaldehyde in the air flow. Experiments were executed in a 200-mlit stirred flow reactor, equipped with a quarts head. This photoreactor was kept in a woody box. 80W Hg lamp was located 3cm above the reactor head as the light source. In Figure 1 main characteristic wavelengths of Hg lamp have been shown with or without UV cutter (HOYA-HMC) that has been used to eliminate UV wavelengths of light source.

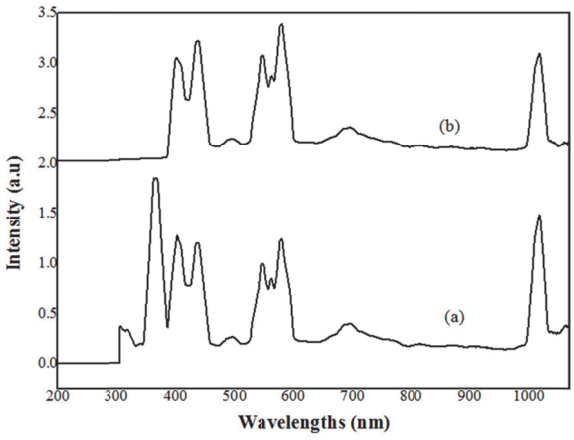

Figure 1. *Characteristic wavelengths of 80W Hg lamp: a) without UV cutter; b) with UV cutter*

At room conditions, a mixture containing 1000 ppm acetaldehyde in air with flow rate of 15mlit/min (which was adjusted with a mass flow controller (MFC)) was fed into the reactor and passed over 0.1g of produced materials. Operational conditions have been brought in Table 1.

Table 1. *The operation conditions for photocatalytic experiments*

Temperature	25°C
Volume of reactor	200 mlit
Light source	80W
Mass of catalysts	0.1 gr
Feed concentration	1000 ppm
Flow rate	15 mlit/min

The reactor was kept in dark until the adsorption cycle completed. Thereafter, the light was turned on and the progress of the reaction was recorded by outlet acetaldehyde concentration using a Gas Chromatograph (VARIAN CP-3800 FID detector GC, column: Propack Q). Figure 2 represents the experimental set up schematically.

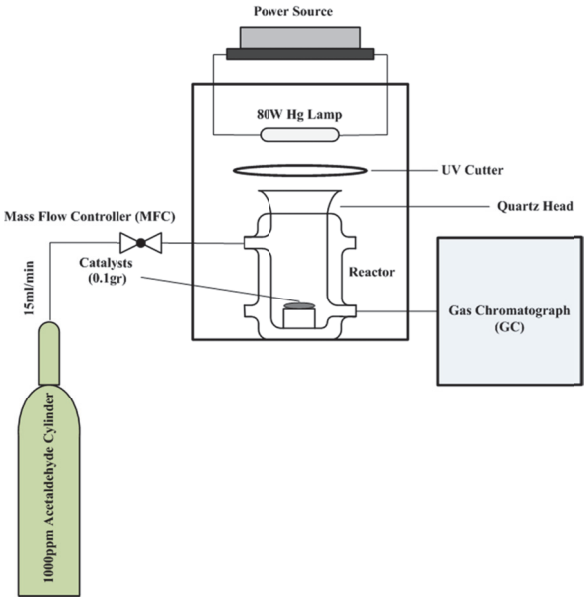

Figure 2. *Experimental set up of photocatalytic tests*

3. RESULTS AND DISCUSSION

3.1. Characterization results

3.1.1. FESEM analysis

Morphologies of bare MWCNT, MWCNT-TiO_2 nanocomposite (NC2) and PT-TiO_2 are shown in Figure 3a, b and c, respectively. Comparison of bare MWCNT surfaces with NC2 indicates the formation of inorganic TiO_2 particles on the outer surface of CNTs. It is clearly observed after excess heat treatment on MWCNT/TiO_2 nanocomposite, tube like structure PT-TiO_2 is formed; however, the presence of agglomerated particles is not under control during the synthesis procedure and weight fractions of primary materials affect the amount of coated and aggregated TiO_2.

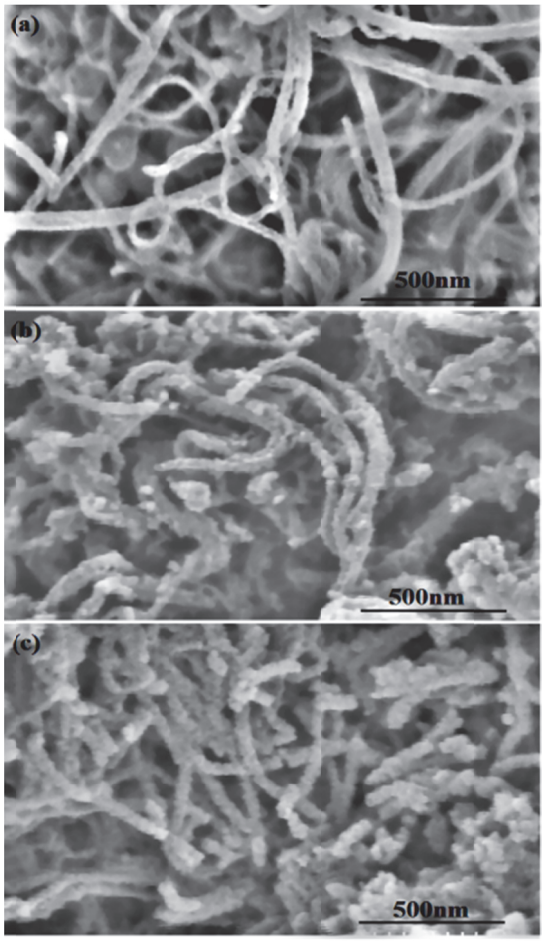

Figure 3. *FESEM images of a) bare MWCNT, b) MWCNT/TiO_2 nanocomposite (NC2), c) pseudo tube TiO_2 (PT-TiO_2)*

3.1.2. X-ray diffraction analysis

The XRD pattern of bare MWCNT is illustrated in Figure 4a. The major diffraction at about

2θ=25.7 is typically corresponding to the (002) graphite. Figure 4b indicates the XRD pattern of P25-TiO_2 where several characteristic peaks at 2θ=25.3, 27.3, 36.0, 37.9, 41.3, 47.9, 53.9, 55.1,62.8, 69, 70.2 and 75 for A(101), R(110), A(103), A(004), R(111), A(200), A(106), A(211), A(204), A(116), A(220) and A(215) diffractions are considered, respectively (A: anatase and R: rutile). According to it, both anatase and rutile crystallites are confirmed in P25-TiO_2 structure but no brukite phase is observed. If the characteristic peaks of NC2 (Figure 4c) are compared with P25-TiO_2, it is easily understood no rutile and brookite crystallites are found and the hybrid material is completely consisted of pure anatase crystals. MWCNT/TiO_2 nanocomposite (NC2) has a distinct peak at 2θ=25.4 that demonstrates (101) anatase phase. Interestingly, main CNT diffraction at 2θ=25.7 is not recognized in the hybrid MWCNT/TiO_2 material. This may be attributed to overlap of the intense peaks of the (002) and (001) reflections and verifies the same conclusion by Gao *et al*. [15]. Similarly, Figure 4d reveals PT-TiO_2 is completely in the form of anatase phase. Formation of pure anatse phase for prepared materials which is validated by XRD results implies that the calcination temperature of 450°C has transformed amorphous TiO_2 to anatase crystallites. Moreover, since both PT-TiO_2 and NC2 are consisted of anatase crystallites, combustion temperature of MWCNTs at 550°C has not changed crystalline arrangement and no transformation of anatase to rutile phase is detected. It is expected the advent of rutile phase begins at about 700°C [17]. The average crystallite size of the synthesized samples was calculated from the XRD data according to the Scherrer's equation [18]:

$$d = \frac{k\lambda}{\beta \cos\theta} \quad (1)$$

where d is the crystallite size, k is a constant (0.9), λ is the wave-length of X-ray (CuKα), β is the half-peak width in radians and θ is the Bragg's diffraction angle in degree. Crystallite size and weight percentage of crystalline phases are listed in Table 2, where as it is considered further thermal treatment to remove MWCNTs have enlarged crystallite size of PT- TiO_2 and this is because of more aggregation of the crystals after thermal treatment at 550°C for 4 hours.

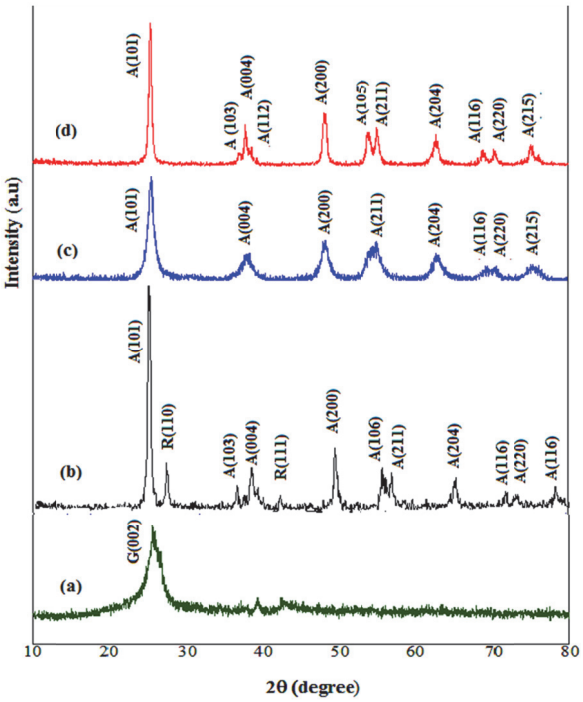

Figure 4. *XRD patterns of (a) bare MWCNT; (b) P25-TiO_2; (c) NC2 and (d) PT-TiO_2*

3.1.3. TGA analysis

TGA analysis was carried out with a ramp rate of 20°C/min in the range of 0-800°C to determine the MWCNT content of NC2. In

Table 2. *Properties of the samples calculated by XRD*

Sample	Anatase (%)	Rutile (%)	Crystallite Size (nm)	d-spacing for (101) plane (Å)
P25-TiO_2	80	20	25	3.52
NC2	100	-	59	3.52
PT-TiO_2	100	-	165	3.51

addition, this experiment was carried out on PT-TiO_2 to investigate the presence of any CNT in the structure. An approximately straight line, parallel to horizontal axis, is observed for PT-TiO_2 in Figure 5a in which it verifies no remarkable change in weight percent. Accordingly, it is deduced that trace amount of MWCNTs is remained in PT-TiO_2 structure. TGA curve of NC2 is represented in Figure 5b.

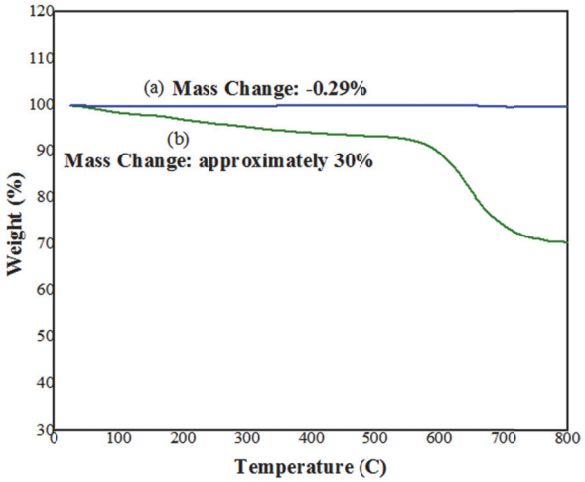

Figure 5. *TGA analysis of (a) PT-TiO2 and (b) NC2*

From 100°C to more than 500°C, a decreasing trend is distinguished due to organic solvent evaporation, TiO_2 network densification and phase transformation from amorphous phase to anatase without detectable weight loss at about 450°C [19].

At the temperature of 520°C, existing MWCNTs begin to burn and finally, approximately 30 percent weight loss is recorded which is almost the same amount of used MWCNT for the synthesis of NC2.

3.1.4. BET analysis

The N_2 adsorption and desorption isotherms of PT-TiO_2 and NC2 are demonstrated in Figure 6a and Figure 6b, respectively. As is clear from the curves, the hysteresis effect is perceived in both samples which can be an evidence for the porous texture of NC2 and PT-TiO_2 samples. In Table 3 the results of BET surface areas and pore volumes of P25-TiO_2, NC2 and PT-TiO_2 are reported.

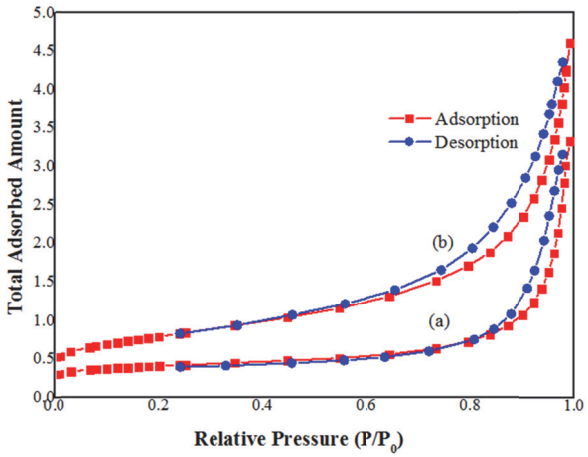

Figure 6. *Adsorption and desorption curves of a) PT-TiO_2 and b) CNT/TiO_2 nanocomposite (NC2)*

Table 3. *BET results of the samples*

Sample	S_{BET} (m^2/gr)	Mean Pore Size (nm)	Pore Volume (cm^3/gr)
P25-TiO_2	43.4	8	0.087
NC2	62.3	9.4	0.146
PT-TiO_2	30.93	13.52	0.104

As expected, pore volumes of NC2 and PT-TiO_2 are greater than P25-TiO_2; whereas negligible difference in pore volume values is observed between NC2 and PT-TiO_2 which mentions NC2 and PT-TiO_2 have similar porous structures. The specific surface area of NC2 is larger than PT-TiO_2 and P25-TiO_2; since, functionalized MWCNTs with benzyl alcohol causes an adequate dispersion and homogenous conjunction with TiO_2 during synthesis, enhancement in pore size and specific surface area are resulted.

In addition, removal of MWCNTs at elevated temperature is led to growth of aggregated particles and reduction in specific surface area.

3.1.5. DRS analysis

The absorption UV-vis spectroscopy of P25-TiO_2, PT-TiO_2 and NC2 are measured and presented in Figure 7. As it is clear in Figure 7a, because of low level absorbance of P25-TiO_2, no remarkable shift to visible light wavelengths is considered. Compared with P25-TiO_2, new absorption edges have been formed for PT-TiO_2 and NC2, according to Figure 7b and Figure 7c,

respectively. In the case of NC2, an excellent ability to absorb wide range of wavelengths is observed.

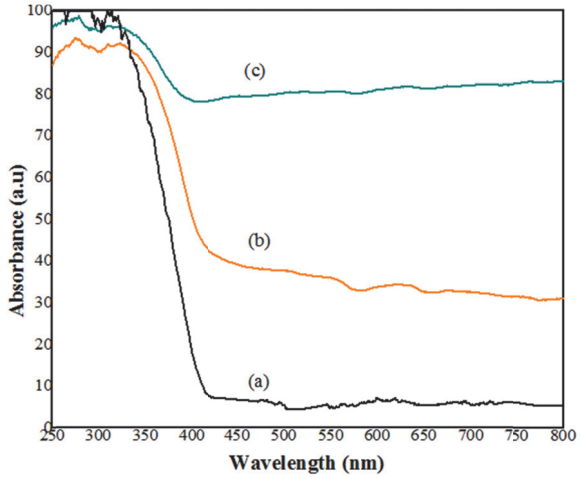

Figure 7. *UV–vis absorption spectra of a) P25-TiO_2, b) PT-TiO_2 and c) NC2*

The diffuse reflectance UV–vis spectra of the different solids expressed in terms of Kubelka-Munk equivalent absorption units are presented for P25-TiO_2 (Figure 8a), PT-TiO_2 (Figure 8b) and NC2 (Figure 8c). Kubelka-Munk function is defined as Equation (2).

$$F(R) = \frac{(1-R)^2}{2R} \qquad (2)$$

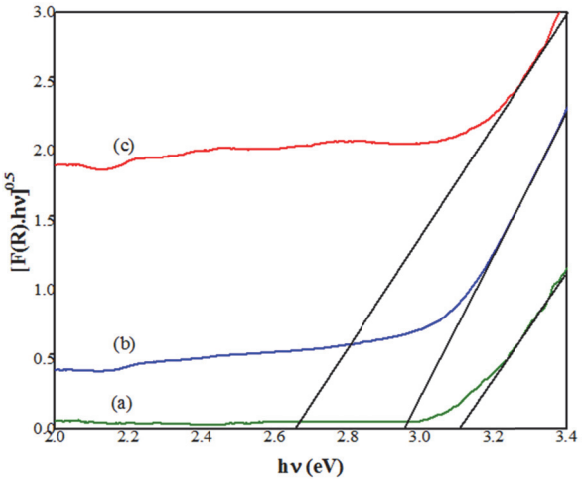

Figure 8. *Kubelka-Munk curves for estimating band gap of the samples: (a) P25-TiO_2; (b) PT-TiO_2 and (c) NC2*

where R is the fraction of reflectance. The band gap of the samples is estimated by extrapolating of a tangent line in the plot of $[F(R).h\upsilon]^{0.5}$ versus the photon energy, hυ (h and υ are the Plank's constant and photon frequency, respectively) [20].

After anticipation of the band gaps, the absorption edges are calculated by the following equation:

$$E_g = \frac{1239.8}{\lambda} \qquad (3)$$

where E_g is the band gap (eV) and λ (nm) is the optical absorption edge. Band gaps and absorption edges of different samples and P25-TiO_2 are exhibited in Table 4.

Table 4. *The band gaps and adsorption edges*

Sample	Band Gap (eV)	Absorption Edge (nm)
P25-TiO_2	3.15	393
NC2	2.67	464.3
PT-TiO_2	2.98	416

3.2. Photocatalytic activity

3.2.1. Results of UV-vis light irradiation

To evaluate the phtocatalytic activity under UV-vis radiation, a continuous flow reactor equipped with 80W mercury light source was used to decompose acetaldehyde as an organic volatile compound (VOC). In Figure 9a photoactivity results of different samples are represented versus time. To prove the existence of photocatalytic activity of the materials, a blank test was performed without any catalyst. The final ability of the samples to degrade VOC is defined as the final conversion which is calculated by:

$$\eta = 1 - \frac{C_{Final}}{C_0} \qquad (4)$$

where C_{Final} is the concentration of acetaldehyde at the end of the process; while C_0 is the initial concentration injected into the reactor (1000ppm acetaldehyde in air). Figure 9b comparatively indicates the conversions of examined materials in terms of bar charts. Albeit in the case of NC2 acceptable degradation efficiency (76%) is resulted during 70 min, but P25-TiO_2 is still showing the highest conversion (88%) under UV-vis radiation. On the other hand, the

conversion by PT-TiO_2 is less significant (26%). It can be said the small size of the crystals as well as combination of 80% anatase and 20% rutile in P25-TiO_2 are the very impressive factors in P25-TiO_2 activity as the superior photocatalytic activity to NC2 under UV-visible light.

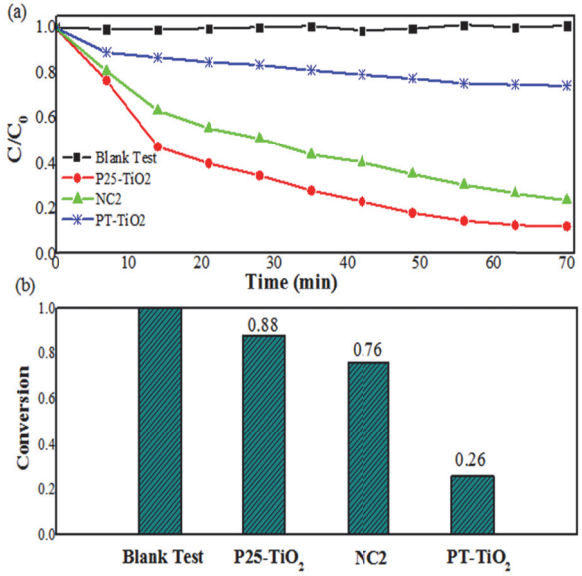

Figure 9. *a) Photocatalytic activity of the samples under UV-vis irradiation; b) Conversion of the samples under UV-vis irradiaton after 70 min at continuous condition*

3.2.2. Results of visible light irradiation

To monitor the photocatalytic activity under visible light, a UV cutter was placed in front of light source to eliminate UV radiation and the process was executed with the same operational conditions as listed in Table 1. Results of photocatalytic performance under visible light irradiation are illustrated in Figure 10a. In Figure 10b conversions of acetaldehyde are expressed by vertical bar charts after 70min exposure to light. About 69% of acetaldehyde is degraded by NC2 after 70 min radiation; whereas 26% of acetaldehyde is decomposed by P25-TiO_2 and only 17% by PT-TiO_2. As considered, under visible light irradiation, the photocatalytic activity of NC2 is well upgraded with respect to P25-TiO_2. It can be said that because most part of photon energy, received by the surface, is in the region of visible light and P25-TiO_2 is inactive under this range of wavelengths, therefore more photoactivity is achieved by NC2 in comparison to P25-TiO_2.

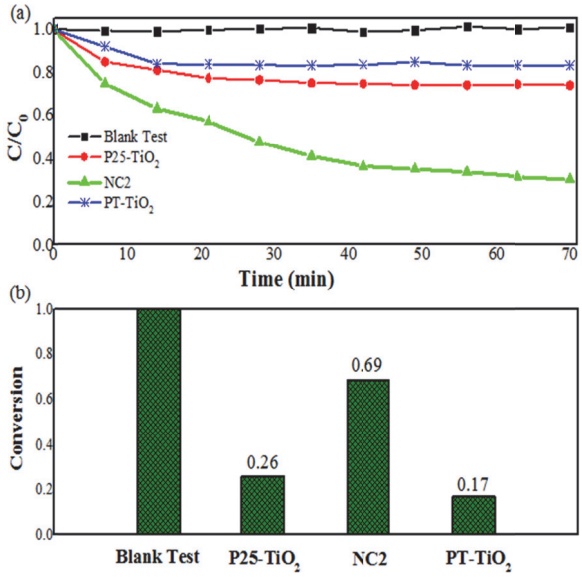

Figure 10. *a) Photocatalytic activity of the samples under visible irradiation; b) Conversions of the samples under visible irradiation after 70 min at continuous condition*

According to above mentioned results, the main conclusions are as following:

a) Results of DRS analysis confirm that in wavelengths below 400 nm, in other words under UV radiation region, the percentage of photon absorption is more. Hence, it is reasonable to say high photoactivity is achieved under UV irradiation toward degradation of VOCs. Hg lamp is consisted of both UV and visible light wavelengths and it is perceived without utilization of UV cutter, both UV and visible light irradiations are concentrated on photocatalysts surfaces. So, compared with being under visible light, greater ability to decompose pollutant is achieved by all examined materials under UV-vis radiation. As it was already mentioned, although remarkable proportion of acetaldehyde is converted by NC2, P25-TiO_2 is still the most photoactive material under UV-visible irradiation. The reason may be realized in the crystalline structure of P25-TiO_2. Prepared materials (NC2 and PT-TiO_2) are consisted of

pure anatase phase; while P25-TiO_2 includes 20% rutile and 80% anatase that grant it unique electronic nature. The anatase phase has a larger photocatalytic activity than the rutile phase and its better performance is attributed to slower recombination rate and better adsorption of inorganic compounds. Accordingly, at first glance, it seems NC2 which is consisted of pure anatase crystallites should have greater photoactivity than P25-TiO_2 with 80% anatase and 20% rutile; but interestingly, whenever the anatase phase is accompanied with the rutile, the photocatalytic activity increased more than even pure anatase. The testimony of this claim is ascribed to charge separation (electron-hole pairs) due to special lattice structure of multiphase P25-TiO_2 [21].

b) Obviously, the existence of CNTs is a reason for enhancement of photocatalytic activity in the visible light region. This is commercially important because UV wavelengths are only a few percent of the solar light source. In general, it is expected that conjunction of TiO_2 with MWCNTs would improve the photocatalytic performance in the three following ways:

1. CNTs can act as dispersing agents which are resulted in enlargement of influential surface area as well as leaves enough active sites for degradation of pollutant molecules [22].

2. CNTs have unique electronic structures that enable them to act as both electron source and sink in presence of TiO_2 that is called "synergistic effect". In Figure 11 synergistic role of CNT with TiO_2 is graphically explained in the photocatalytic process. As shown in Figure 11a, like metal-semiconductor junction, CNT/TiO_2 nanocomposite is led to the formation of a space-charge region called Schottky barrier. Naturally, at the interface of the two materials, electrons migrate from a higher to a lower Fermi level.

Equalized Fermi level is reached at the end of the process. TiO_2 is an n-type semiconductor and incorporation with CNTs would lead the flow of electrons to the CNTs surfaces. In this situation, the CNTs are acting as electron sinks and TiO_2 is turned to a p-type semiconductor. Here, a high-energy photon excites an electron from the valence band to the conduction band of anatse TiO_2. Photogenerated electrons in the space-charge region migrate to the CNTs surfaces and leave holes in the valence band in which redox reactions take part to remove the VOC molecules via creating hydroxyl radicals [23].

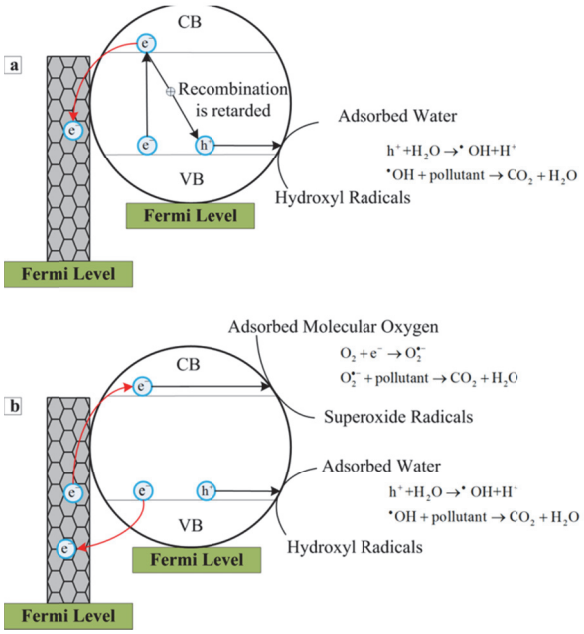

Figure 11. *Synergistic effect of CNT; a) electron sink, b) electron source*

3. Aside acting as electron sinks, the CNTs are counted as photosensitizers or electron sources. In Figure 11b, with the absorption of energetic photons by bare CNTs, the photogenerated electrons are injected to the conduction band of TiO_2 allowing for formation of the superoxide radicals from adsorbed molecular oxygen. Now, positively charged CNTs separate electrons from the valence band and leave holes which is led to reaction with adsorbed water to form hydroxyl radicals [23].

c) DRS analysis proves that photoabsorption of PT-TiO_2 is shifted to the visible light region. Comparing its band gap (2.98eV) and absorption edge (416 nm) with respective values of P25-TiO_2 (3.15eV and 393 nm) indicates modification of optical and electronic structure of PT-TiO_2. Reduction of PT-TiO_2 electronic

band gap is favorable for the photocatalytic activity under visible light region but as it is realized from the photocatalytic experiments, negligible activity is estimated for PT-TiO_2. The extra heat treatment of NC2 for combustion of MWCNTs is propelled the particle size to enlarge significantly through the irregular agglomeration. Therefore, as it is certified by BET analysis, reduction of the specific surface area occurred for PT-TiO_2 in comparison with other samples (Table 3). Additionally, from Scherrer formula, average crystal size of PT-TiO_2 is very large and it adversely affects the photocatalytic efficiency. Hence, according to estimated electronic band gap and absorption edge by DRS analysis, it is revealed that optical and electronic properties are not responsible for the low photocatalytic activity of PT-TiO_2. Indeed, conforming to BET and XRD results, lack of enough active sites due to the large crystal sizes and reduction of influential surface area are the reasons of low photoactivity of PT-TiO_2.

3.3. Evaluation of loaded MWCNT on acetaldehyde conversion

The effect of loaded fraction of MWCNT in photocatalytic activity of MWCNT/TiO_2 was investigated using three different ratios of MWCNT (20, 30 and 40 wt%) in the prepared samples, and the results are observed in Figure 12a and Figure 12b. Initially, it seems that more increase in MWCNT fraction means more photocatalytic conversion, whereas according to the recorded results, the highest photoactivity belongs to NC2 with 30 wt% MWCNT. Possibly, the less coated fraction of TiO_2 on the side walls at high fraction of MWCNT results in reduction of photo excitation of electrons under light irradiation. On the other hand, the high fraction of TiO_2 may cause accumulation of nano TiO_2 particles on the surface of CNT and decrease the assistance of CNT in photocatalytic excitation under visible light.

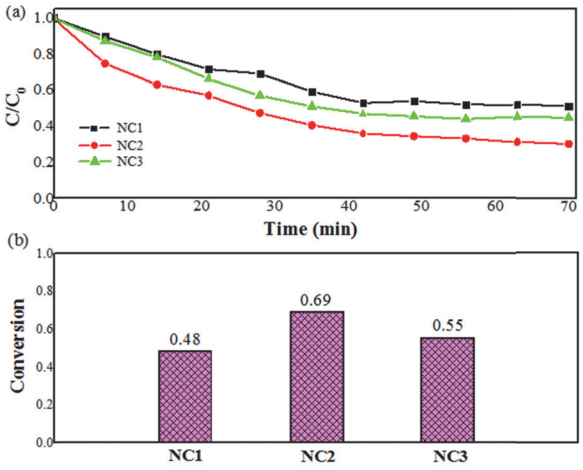

Figure 12. *a) Effect of CNT loading; b) Conversions of the samples under visible irradiation after 70 min at continuous condition*

4. CONCLUSION

MWCNT/TiO_2 nanocomposite was synthesized by a facile surfactant aided sol-gel method at normal temperature and pressure. The MWCNT was removed under secondary thermal treatment to obtain PT-TiO_2 structure. The remained product after thermal treatment was a mixture of pseudo-tube and agglomerated TiO_2 crystals in which the fraction of tube structures to the nano particles was influenced by the stoichiometry of primary materials used in the synthesis gel. Photoactivity of the materials was examined to degrade acetaldehyde in a stirred flow reactor and the results were compared with P25-TiO_2 activity. Although under UV-vis irradiation P25-TiO_2 was the most active photocatalyst (with 87% acetaldehyde conversion), in the visible light region, nanocomposite MWCNT/TiO_2 with anatase phase structure showed the most improvement in photocatalytic activity and led to appropriate efficiency of removing organic pollutants. It was concluded that an optimum amount of MWCNT with anatase TiO_2 would be required to enhance the photocatalytic activity of TiO_2 toward visible light irradiation. On the other side, the thermal treated pseudo-tube TiO_2 could not show remarkable photoactivity under visible light irradiation. This poor performance was attributed to agglomeration under heat treatment and reduction influential surface area, as well as absence of CNT from the structure of the produced material.

REFERENCES

1. A. Fujishima, X. Zhang and D.A. Tryk: TiO_2 photocatalysis and related surface phenomena, Surf. Sci. Rep., Vol: 63, (2008), pp. 515-582.
2. Y.J. Xu, Y. Zhuang and X. Fu: New insight for enhanced photocatalytic activity of TiO_2 by doping carbon nanotubes: a case study on degradation of benzene and methyl orange, J. Phys. Chem C., Vol: 114, (2010), pp. 2669-2676.
3. M. Pelaez, N.T. Nolan, S.C. Pillai, M.K. Seery, P. Falaras, A.G. Kontos, P.SM Dunlop, J.WJ Jeremy, J.A. Byrne and K. O'Shea: A review on the visible light active titanium dioxide photocatalysts for environmental applications, Appl. Catal B: Environ., Vol.125, (2012), pp.331-349.
4. R. Leary and A. Westwood: Carbonaceous nanomaterials for the enhancement of TiO_2 photocatalysis, Carbon., Vol. 49, (2011), pp. 741-772.
5. Q. Cao, Q. Yu, D.W. Connell and G. Yu: Titania/carbon nanotube composite (TiO_2/CNT) and its application for removal of organic pollutants, Clean. Tech. Environ. Policy., Vol. 15, (2013), pp. 871-880.
6. D. Eder: Carbon nanotube− inorganic hybrid". Chem, Rev., Vol. 110, (2010), pp. 1348-1385.
7. Y. Yu, J.C. Yu, J.G. Yu, Y.C. Kwok, Y.K. Che, J.C. Zhao, L. Ding, W.K. Ge and P.K. Wong: Enhancement of photocatalytic activity of mesoporous TiO_2 by using carbon nanotubes, Appl. Catal A: Gen., Vol. 289, (2005), pp. 186-196.
8. W. Wang, P. Serp, P. Kalck and J.L. Faria: Photocatalytic degradation of phenol on MWNT and titania composite catalysts prepared by a modified sol–gel method, Appl. Catal B: Environ., Vol. 56, (2005), pp. 305-312.
9. S.M. Miranda, G.Em Romanos, V. Likodimos, R. Marques, E.P. Fawas, F.K. Katsaros, K.L. Stefanopoulos, V.JP. Vilar, J.L. Faria and P. Falaras: Pore structure, interface properties and photocatalytic efficiency of hydration/dehydration derived TiO_2/CNT composites, Appl. Catal B: Environ., Vol. 147, (2014), pp. 65-81.
10. Y. Li, L. Li, C. Li, W. Chen and M. Zeng: Carbon nanotube/titania composites prepared by a micro-emulsion method exhibiting improved photocatalytic activity, Appl. Catal A: Gen., Vol. 427, (2012), pp. 1-7.
11. K.H. Ji and D.M. Jang: Comparative photocatalytic ability of nanocrystal-carbon nanotube and-TiO_2 nanocrystal hybrid nanostructures, J. Phys. Chem C., Vol. 113, (2009), pp. 19966-19972.
12. J. Sun, M. Iwasa, L. Gao and Q Zhang: Single-walled carbon nanotubes coated with titania nanoparticles, Carbon., Vol. 42, (2004), pp. 895-899.
13. D. Tasis, N. Tagmatarchis, A. Bianco, and M. Prato: Chemistry of carbon nanotubes, Chem. Rev., Vol. 106, pp. 1105-1136.
14. V.R. Djokić, A.D. Marinković, O. Ersen, P.S. Uskoković, R.D. Petrović, V.R. Radmilović, and D.T. Janaćković: The dependence of the photocatalytic activity of TiO_2/carbon nanotubes nanocomposites on the modification of the carbon nanotubes, Ceram. Int., Vol. 40, (2014), pp. 4009-4018.
15. B. Gao, G.Z. Chen, and G.Li. Puma: Carbon nanotubes/ titanium dioxide (CNTs/TiO_2) nanocomposites prepared by conventional and novel surfactant wrapping sol–gel methods exhibiting enhanced photocatalytic activity, Appl. Catal B: Environ., Vol. 89, (2009), pp. 503-509.
16. D.J. Cooke, D. Eder and J.A. Elliott: Role of benzyl alcohol in controlling the growth of TiO2 on carbon nanotubes, J. Phys. Chem C., Vol. 114, (2010), pp**.** 2462-2470.
17. N. Bouazza, M. Ouzzine, M.A. Leo-Rodenas, D. Eder and A. Linares-Solano: TiO_2 nanotubes and CNT–TiO_2 hybrid materials for the photocatalytic oxidation of propene at low concentration, Appl. Catal B: Environ., Vol. 92, (2009), pp. 377-383.
18. O. Carp, C. Huisman and A. Reller: Photoinduced reactivity of titanium dioxide, Prog. Solid. State. Chem., Vol. 32, (2004), pp. 33-177.
19. D. Eder and A.H. Windle: Morphology control of CNT-TiO_2 hybrid materials and rutile nanotubes, J. Mater. Chem., Vol. 18, (2008), pp. 2036-2043.
20. Y.I. Kim, S.J. Atherton, E.S. Brigham and T.E. Mallouk: Sensitized layered metal oxide semiconductor particles for photochemical hydrogen evolution from nonsacrificial electron donors, J. Phys. Chem B., Vol. 97, (1993), pp. 11802-11810.
21. D.C. Hurum, A.G. Agrios, K.A. Gray, T. Rajh and M.C. Thurnauer: Explaining the enhanced photocatalytic activity of Degussa P25 mixed-phase TiO_2 using EPR, J. Phys. Chem B., Vol. 107, (2003), pp. 4545-4549.
22. K. Woan, G. Pyrgiotakis and W. Sigmund: Photocatalytic Carbon-Nanotube– TiO_2

Composites, Adv. Mater., Vol. 2, (2009), pp. 2233-2239.

23. Z. Liu, Q. Zhang and L.C. Qin: Reduction in the electronic band gap of titanium oxide nanotubes, Solid State Commun.,Vol. 14, (2007), pp. 168-171.